

# Proposal for measuring the quantum states of neutrons in the gravitational field with a CCD-based pixel sensor

T. Sanuki<sup>\*,a</sup>, S. Komamiya<sup>b,c</sup>, S. Kawasaki<sup>b</sup>, S. Sonoda<sup>b</sup>

<sup>a</sup>*Graduate School of Science, Tohoku University, Sendai-shi, Miyagi 980-8578, Japan*

<sup>b</sup>*Graduate School of Science, The University of Tokyo, Bunkyo-ku, Tokyo 113-0033, Japan*

<sup>c</sup>*International Center for Elementary Particle Physics, The University of Tokyo, Bunkyo-ku, Tokyo 113-0033, Japan*

---

## Abstract

An experimental setup is proposed for the precise measurement of the quantum states of ultracold neutrons bound in the earth's gravitational field. The experiment utilizes a CCD-based pixel sensor and magnification system to observe the fine structure of the neutron distribution. In this work, we analyzed the sensor's deposited energy measurement capability and found that its spatial resolution was  $5.3 \mu\text{m}$ . A magnifying power of two orders of magnitude was realized by using a cylindrical rod as a convex mirror.

*Key words:* neutron, quantum state, gravitational field, CCD

---

## 1. Introduction

The energy of a neutron is quantized when it is bound in the earth's gravitational field. As a consequence, the vertical distribution will not be smooth; rather, the distribution will exhibit modulation. The scale of this density modulation is calculated to be  $(\hbar^2/2m_n^2g)^{1/3} \sim 6 \mu\text{m}$ , where  $m_n$  is the neutron mass. Such quantum states have recently been observed in [1, 2, 3]. A more precise measurement of these quantum states can be used to verify the validity of the gravitational equivalence principle and search for new short-range forces.

---

\*Corresponding author. Tel.:+81-22-795-6727; fax:+81-22-795-6728  
*Email address:* sanuki@awa.tohoku.ac.jp (T. Sanuki)

In the previous experiment, the vertical spatial density of neutrons was observed by using a uranium-coated plastic nuclear track detector (CR39). The detector’s spatial resolution was estimated to be as high as  $\sim 2\ \mu\text{m}$  by observing the distribution of neutrons [3]. Since temporal information is not recorded in such plastic nuclear track detectors, these detectors are intolerable to accidental events and background signals. We believe that a pixel detector with a real-time readout is an ideal device for precisely measuring positions in applications with low event rates.

Silicon pixel sensors, such as CCDs, can measure both the spatial and temporal position of charged particles as the particles pass through the sensor. With the addition of a coating that converts neutron events into charged particle events that may be observed with the CCD, the position of the original neutron event can be determined very precisely and in almost real time. We have developed such a “fine-pixel neutron detector,” which is based on commercially available CCD technology.

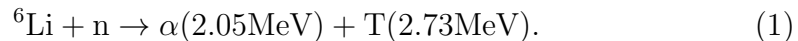
In order to observe the structure of the neutron density modulation at scales much smaller than the size of a CCD pixel, we have designed and demonstrated a simple magnification system. Our system uses a cylindrical rod as a convex mirror that can stretch the small modulation pattern of the neutron distribution by a factor of 40 or more.

In the following we propose an experimental setup that may be used to precisely measure the quantum states of ultracold neutrons bound in the earth’s gravitational field.

## 2. CCD-based neutron detector

### 2.1. CCD sensor

In order to detect neutrons with a CCD sensor, the sensor needs to be coated with a neutron converter, like  ${}^6\text{Li}$ , which produces charged particles via the following process:



The resulting alpha particle and triton can penetrate through silicon to characteristic depths of  $8\ \mu\text{m}$  and  $40\ \mu\text{m}$ , respectively. If there is thick, insensitive material in front of the CCD sensitive volume the charged particles that are produced will not be able to enter the sensitive volume. Therefore, back-thinned CCD is ideal for neutron detection. In our study a S7170-0909

(Hamamatsu Photonics K.K.) was selected for its wide active area and pixel size. Other specifications of this CCD are listed in Table 1.

Table 1: Specifications of the CCD S7170-0909 ( $T_a = 25^\circ\text{C}$ ).

Parameter	
Active Area	$12.288 \times 12.288$ mm
Number of Pixels	$512 \times 512$
Pixel Size	$24 \times 24$ $\mu\text{m}$
Frame Rate	0.9 frames/s
Spectral Response Range	200 to 1100 nm
Full Well Capacity (Vertical)	$300 ke^-$
Dark Current Max. $0^\circ\text{C}$	$600 e^-/\text{pixel/s}$
Readout Noise	$8 e^-$ rms

## 2.2. Neutron converter

Since the secondary charged particles are emitted isotropically from the neutron conversion point, these particles can be produced at a large incident angle with respect to the CCD surface. For events of this kind, the position detected is shifted from the position where the particle is emitted, reducing the spatial resolution of the detector if there is a gap between the CCD and the neutron conversion point. In order to determine a neutron's incident position precisely, the neutron-converter layer should be very thin and should be attached directly to the CCD so that the secondary charged particles enter the CCD immediately after the nuclear reaction.

In our design, the neutron converter is formed directly on the CCD and the thickness is much less than the size of the CCD pixels  $24 \mu\text{m}$ . The converter was processed using the vacuum evaporation facility at the Kyoto University Research Reactor Institute (KURRI) in Japan [4, 5]. A  $0.09 \mu\text{g}/\text{cm}^2$  (20 nm) Ti layer was formed on the CCD, providing an adhesive surface. A  ${}^6\text{Li}$  layer of  $0.11 \mu\text{g}/\text{cm}^2$  (230 nm) was then formed on the Ti layer to function as a neutron converter. The  ${}^6\text{Li}$  converter was covered with a  $0.09 \mu\text{g}/\text{cm}^2$  (20 nm) Ti layer to prevent the  ${}^6\text{Li}$  layer from reacting with moisture in the atmosphere.

### 2.3. Energy measurement

In order to investigate the feasibility of using a CCD for neutron detection, the CCD coated with a neutron converter was irradiated with cold neutrons at the MINE2 beam line of the research reactor JRR-3M of the Japan Atomic Energy Agency (JAEA); the neutron wavelength was 0.88 nm. The detection efficiency for cold neutrons was measured to be 0.3 %, consistent with the efficiency estimated from a cross-section of the nuclear reaction (1) and the thickness of the  ${}^6\text{Li}$  converter. The efficiency corresponds to 13 % for ultracold neutrons, where the cross-section is inversely proportional to velocity. To detect ultracold neutrons more efficiently, a thicker  ${}^6\text{Li}$  layer is required in the neutron converter.

Fig. 1 shows an example of charge distribution in the CCD pixels for one event. A secondary charged particle loses its energy inside the CCD and creates as many as  $10^6$  electron-hole pairs. Due to diffusion inside the silicon, the electrons created during ionization are distributed in neighboring pixels to form a cluster.

The total charge inside the cluster is proportional to the energy deposited by the incoming particle. A correlation between the total charge and the total energy deposited was calibrated using an alpha source  ${}^{241}\text{Am}$ . The alpha source and the CCD were first placed inside a vacuum chamber; the distance between them was 122.6 mm. Then the chamber was filled with dry  $\text{N}_2$  gas and the pressure varied between  $3.0 \times 10^4$  Pa and  $2.4 \times 10^2$  Pa. The energy loss between the alpha source and the CCD depends on the amount of material between them. Here, the energy of the alpha particle at the CCD varied between 0.001 MeV and 4.75 MeV. The energy of the event, shown in Fig. 1, was calculated to be 2.0 MeV.

Fig. 2 shows the energy spectrum obtained at the MINE2 cold neutron beam line. It clearly shows the two peaks around 1.8 MeV and 2.5 MeV, which correspond to the alpha particles (2.05 MeV) and the tritons (2.73 MeV), respectively. The observed energy is slightly smaller than the expected value because the charged particles lose a fraction of their energy in the converter and the insensitive volume of the CCD. Fig. 2 shows another peak around 0.9 MeV, which decreases gradually with increasing energy, but has a sharp edge on the lower energy side. This spectral shape is caused by tritons that are energetic enough such that their range is longer than the thickness of the CCD sensitive volume. Supposing that the tritons stopping power (energy loss rate) is constant throughout the CCD, the energy deposited inside of the CCD sensitive volume,  $E$ , is a function of the incident angle  $\theta$  as

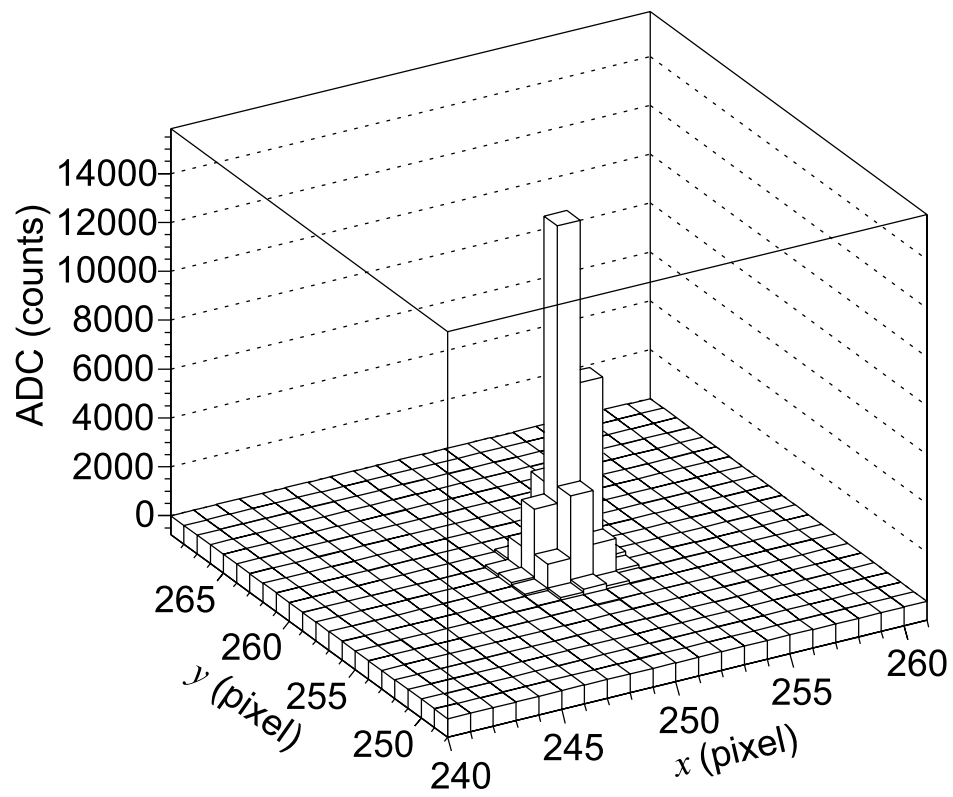


Figure 1: Typical observed event.

$E = t\rho\epsilon/\cos\theta$ , where  $t$  is the thickness of the CCD sensitive volume,  $\rho$  is the density of the silicon, and  $\epsilon$  is the stopping power ( $\epsilon \equiv -dE/dx$ ). Since the secondary particles are emitted isotropically, the number of events  $dN(\theta)$  in between  $\theta$  and  $\theta + d\theta$  is proportional to  $2\pi \sin\theta d\theta$ . The shape of the energy spectrum will be like  $dN/dE \propto E^{-2}$ ; an inverse-square shape that should have upper and lower limits. For incident particles with an initial energy  $E_0$ , all events with an incident angle larger than  $\cos^{-1}(t\rho\epsilon/E_0)$  will be accumulated at  $E_0$ , resulting in a peak. The lower edge of the deposited energy corresponds to the vertically incident particles. The deposited energy is equal to  $t\rho\epsilon$ , which amounts to about 0.9 MeV in our experiment.

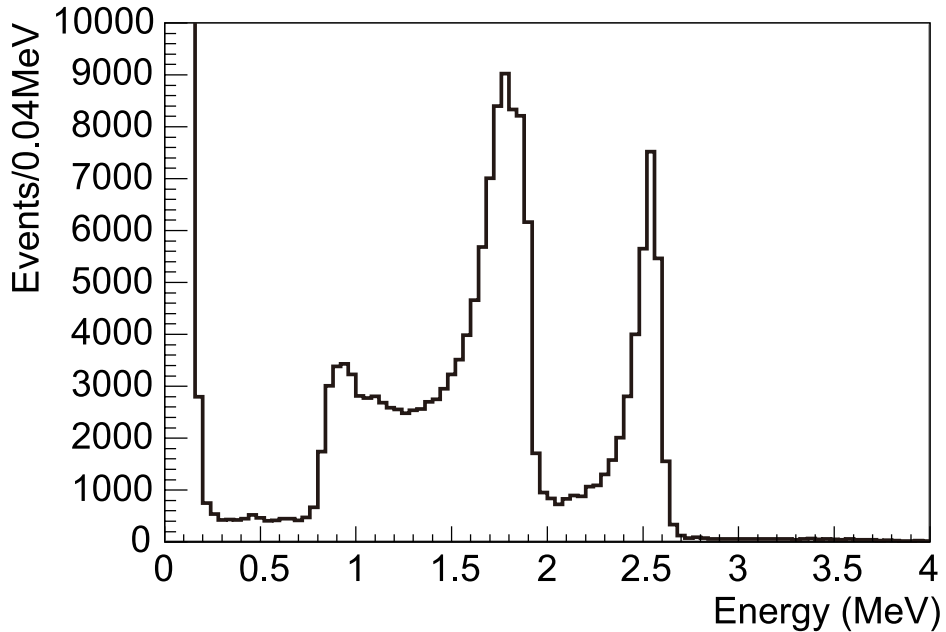


Figure 2: Energy spectrum observed with the CCD coated with  ${}^6\text{Li}$ .

The distribution of the energy lost inside the converter and the CCD insensitive volume will have the same inverse-square shape as the distribution inside the CCD sensitive volume described above. Therefore, each peak, corresponding to the alpha particles and tritons that stop inside the CCD, has a tail proportional to  $(E_0 - E)^{-2}$  on the low energy side. The shape of this tail is blurred since the distance between the neutron conversion point and the CCD surface can vary between zero and the full thickness of the

converter.

#### 2.4. Position measurement

The electrons spread out over the pixels, as shown in Fig. 1, due to diffusion inside the silicon. The barycenter of the charge gives a finer hit-point than the pixel size.

A reference pattern was produced with a gadolinium foil to estimate the hit-position resolution for neutrons. The thickness of the foil is  $25\ \mu\text{m}$ , which is thick enough to fully absorb cold neutrons. The 144 fine spoke-like slits shown in Fig. 3(a) were produced with an excimer laser by Laserx CO.LTD. Each of the spoke-like slits has four trapezoidal holes, as shown in Fig. 3(b). The reference pattern was placed just in front of the  ${}^6\text{Li}$ -coated CCD. The distance between the pattern and the CCD was as small as  $150\ \mu\text{m}$ . The CCD and reference pattern were exposed to cold neutrons at the MINE2 beam line of the research reactor JRR-3M. The pattern was then projected onto the CCD.

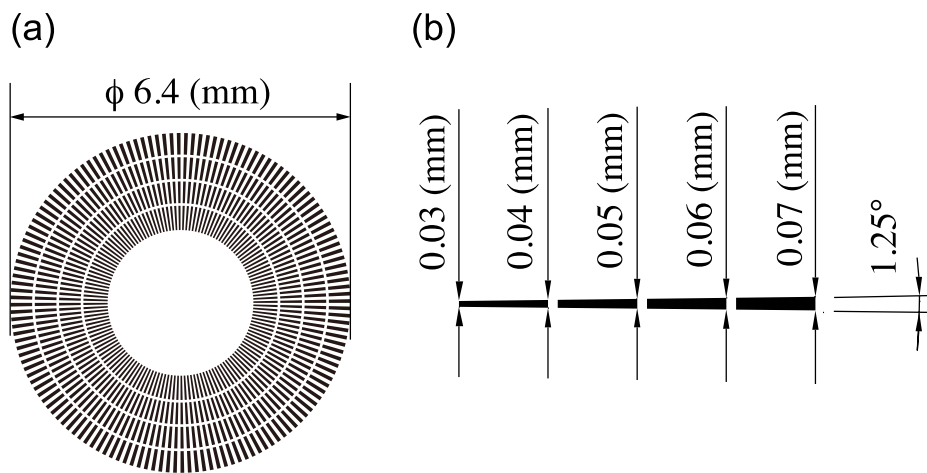


Figure 3: (a) The reference pattern used for the resolution measurement, and (b) a close-up view of one “spoke.”

Fig. 4 shows hit-position distributions for the alpha particles and tritons. These distributions are estimated by calculating the barycenter of the deposited charge. In order to select alpha particles and tritons, the amount of energy deposited in each event was required to be in the range of  $1.4\ \text{MeV} - 2.0\ \text{MeV}$  and  $2.2\ \text{MeV} - 2.7\ \text{MeV}$ , respectively. All of the events are plotted

in an octant area, assuming that the event distribution has an 8-fold rotational symmetry. For the tritons, we were not able to see a pattern along the innermost part of the fan shape. This is because the tritons have a long range inside of the CCD. On the other hand, a clear pattern can be seen for the alpha particles. The hit-position distribution for alpha particles suggests that a spatial resolution of better than  $30\ \mu\text{m}$  was achieved.

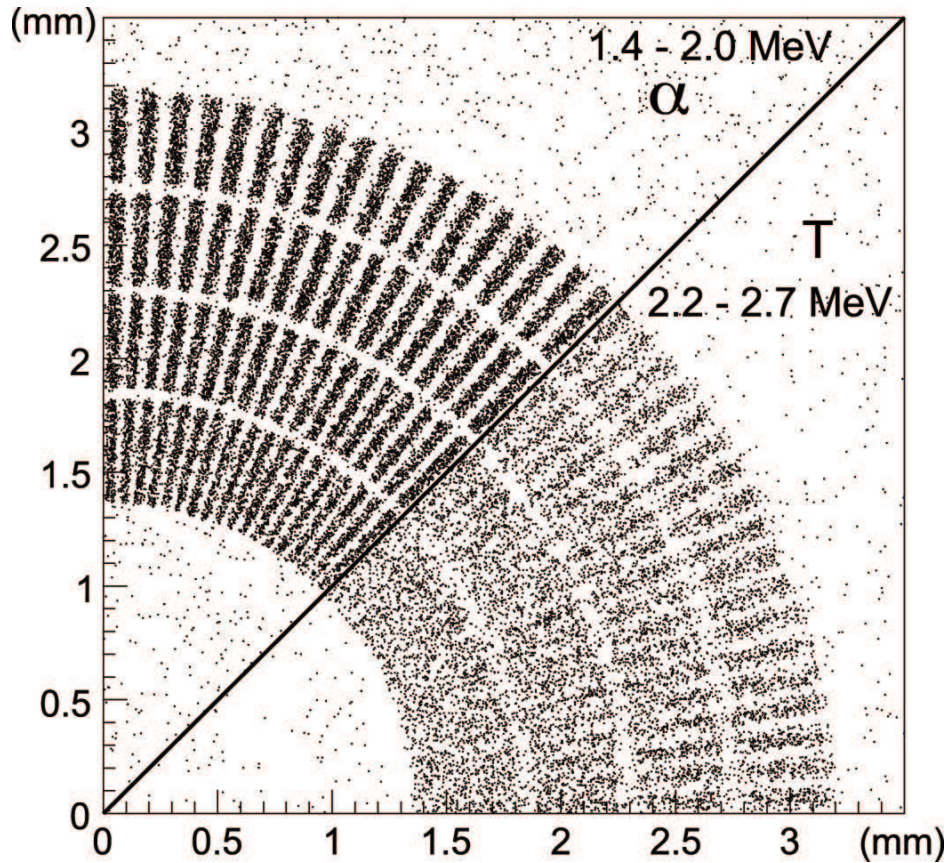


Figure 4: The hit-position distribution of the alpha particles and the tritons.

In order to estimate the spatial resolution more precisely, the distances between the calculated hit-positions and the edge of the slit was examined. Fig.5 shows the distribution of these distances for alpha particles. This



distribution can be expressed as,

$$f(x) = p_1 \cdot \operatorname{erf} \left( \frac{x}{\sqrt{2}\sigma} + p_2 \right) + p_3, \quad (2)$$

where  $x$  is the distance,  $\sigma$  corresponds to the spatial resolution, and  $p_1$ ,  $p_2$  and  $p_3$  are fitting parameters. The estimated spatial resolution was  $5.3 \pm 0.3 \mu\text{m}$  for alpha particles. This is 4.5 times smaller than the CCD pixel size.

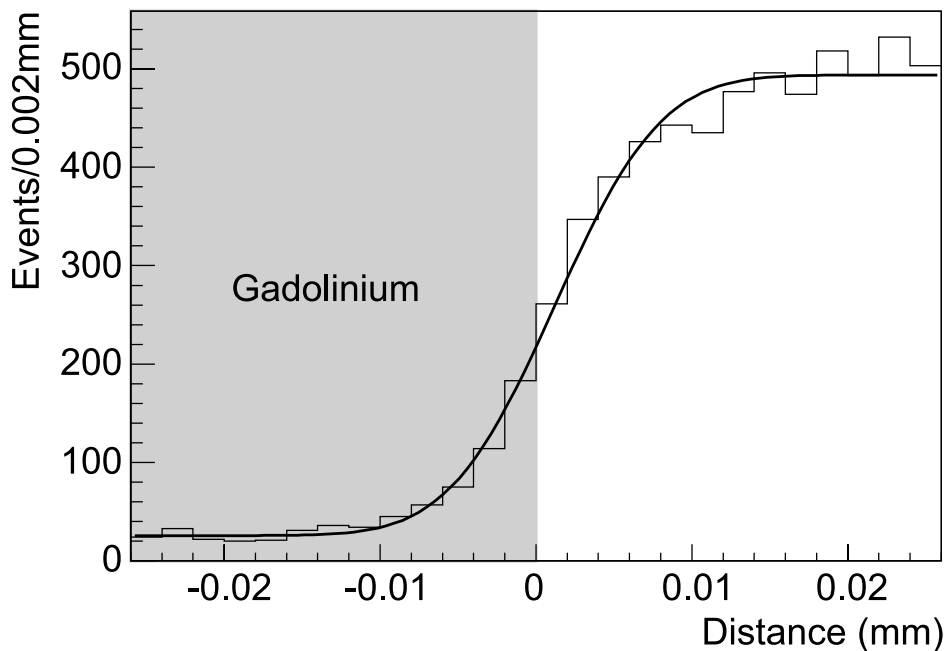


Figure 5: The distance between the hit-position and the edge of the slit.

Our examination of the reference pattern via optical microscopy shows that the slits in the reference pattern were not perfectly straight. This is probably because the gadolinium foil was too thick to make slits as narrow as  $30 \mu\text{m}$ . The variations from a straight slit edge were observed to be  $1\text{--}2 \mu\text{m}$ . The slit pattern had other imperfections as well: the slit walls were not strictly perpendicular to the face surface. Our estimation of the detector resolution would be slightly worsened by both of these effects.

### 3. Application to ultracold neutron experiment

A neutron's energy is quantized when it is bound in the earth's gravitational field. Given this effect, we expect to observe a modulation in the vertical distribution of neutrons in terrestrial experiments. The scale of this modulation is about  $6 \mu\text{m}$ , so a magnification system is needed to observe the modulation with a CCD-based neutron detector whose spatial resolution is around  $5 \mu\text{m}$ .

A cylinder is used as a convex mirror to magnify the small modulation pattern of the neutron distribution, as shown in Fig. 6. The cylinder converts horizontal velocity into vertical velocity, after which the neutrons escape from the earth's gravitational field and follow their classical trajectories.

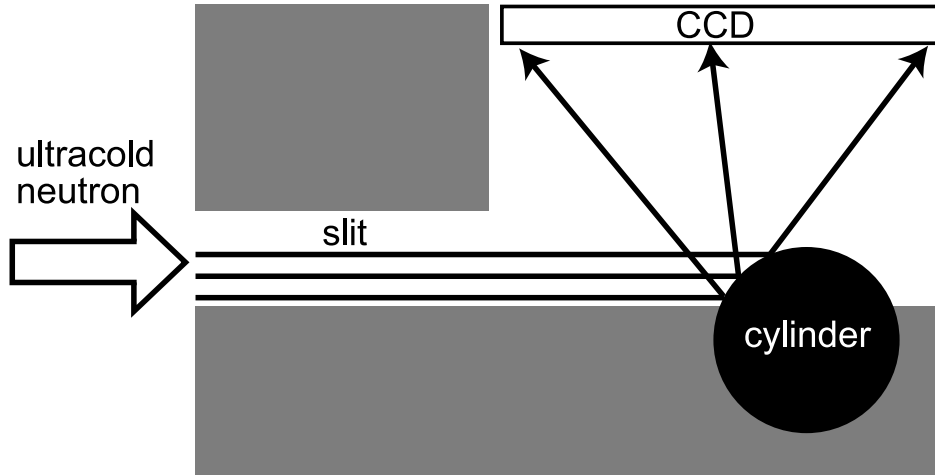


Figure 6: An experimental setup (not to scale).

The magnification was demonstrated by observing a magnified laser interference fringe pattern with the CCD. When two coherent laser beams intersect at an angle  $\phi$ , they produce a pattern of interference fringes. The fringe spacing is given by  $\lambda/2 \sin(\phi/2)$ , where  $\lambda$  is the wavelength of the laser light [6, 7]. This fringe pattern was magnified with the cylinder and then observed with the CCD. A layout of the optical components we used is shown in Fig. 7. In our demonstration, a green Nd:YAG laser ( $\lambda=532 \text{ nm}$ ) was used and the angle of intersection was measured to be  $0.0722 \pm 0.0003$  radian, resulting in a fringe spacing of  $7.37 \pm 0.03 \mu\text{m}$ . The diameter of the cylinder

was 1.5 mm, and the distance between the center of the cylinder and the CCD was designed to be 11.25 mm.

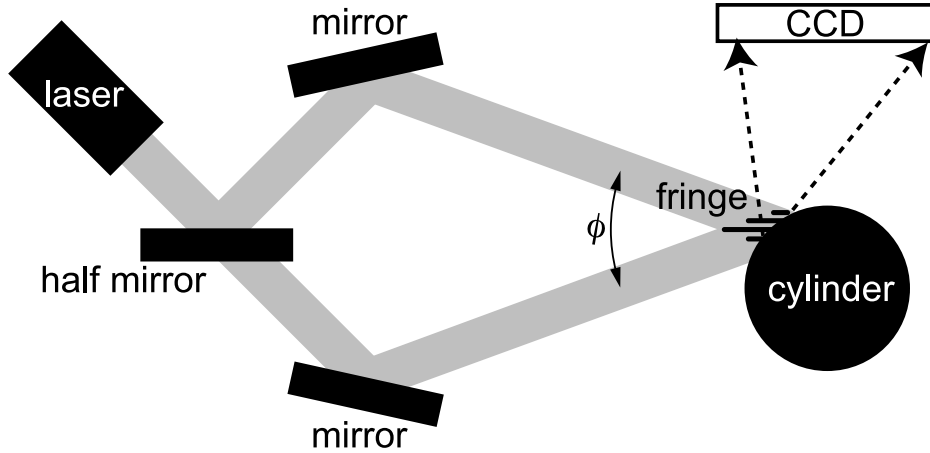


Figure 7: The layout of the optical components used in the magnification demonstration. (not to scale)

Fig. 8(a) shows the fringe pattern observed with the CCD. The observed intensity distribution was reproduced in a calculation, shown in the figure by the white curve. The magnifying power was calculated to be 40 – 200 from the observed fringe spacing on the CCD, as shown in Fig. 8(b). The error in the estimated magnifying power is mainly due to uncertainty in determining the peak positions of the fringe pattern. The horizontal error bars show the distance between the adjacent fringes. Fig. 8 shows that the magnification system functions as designed. These results demonstrate that with this simple magnification system, where a single cylinder is used as a convex mirror, an effective spatial resolution of  $0.1 \mu\text{m}$  can be achieved combined with the CCD-based neutron detector.

In order to precisely measure the position of the ultracold neutrons, we need to further optimize the material of the cylinder, as well as its diameter and distance to CCD. In order to fully understand the magnification system and precisely estimate the neutron distribution shown by the CCD, it would be needed to calculate the evolution of the neutron wave function for the specific experimental situation of our measurement.

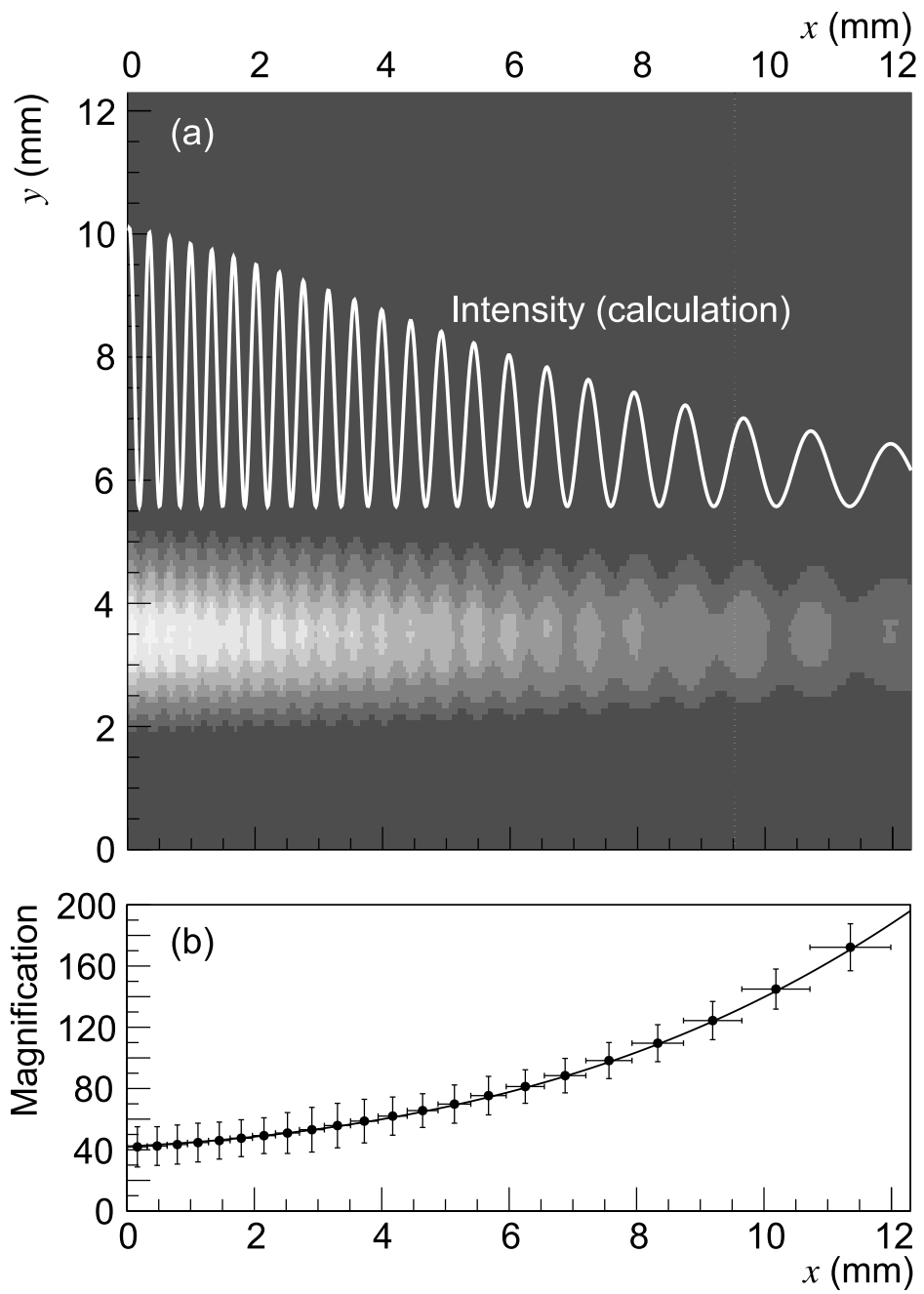


Figure 8: (a) Magnified fringe pattern observed with the CCD, and (b) the obtained magnification power. The calculated intensity is superimposed as a white line in (a).

## 4. Summary

We developed a CCD-based pixel sensor for measuring neutrons. A sufficient energy measurement capability and a spatial resolution of  $5.3 \mu\text{m}$  were demonstrated using the cold neutrons at the MINE2 beam line of the JRR-3M research reactor. We propose that this sensor can be used to observe the quantum states of neutrons bound in the earth's gravitational field. The neutron density modulation pattern can be stretched by two orders of magnitude using a simple magnification system composed of a cylindrical neutron reflector of 1.5 mm in diameter. We have demonstrated that the fine structure of the neutron density modulation can be clearly observed using the proposed CCD-based detector coupled to the cylinder-based magnification system.

## 5. Acknowledgements

We are indebted to Prof. M. Hino and Dr. M. Kitaguchi from Kyoto University Research Reactor Institute (KURRI), and Prof. H.M. Shimizu and Prof. Y. Higashi from High Energy Accelerator Research Organization (KEK) for their technical support and encouragement. We thank Dr. Y. Kamiya, Mr. H. Okawa and Mr. N. Mori from The University of Tokyo for their support. This work was partially supported by KAKENHI (18340056) and Grant-in-Aid for JSPS Fellows (19-4404).

## References

- [1] V. V. Nesvizhevsky, et al., *Nature* 415 (2002) 297–299.
- [2] V. V. Nesvizhevsky, et al., *Phys. Rev. D* 67 (2003) 102002.
- [3] V. V. Nesvizhevsky, et al., *Eur. Phys. J. C* 40 (2005) 479–491.
- [4] T. Ebisawa, et al., *Nucl. Inst. Methods A* 350 (1994) 296–299.
- [5] S. Tasaki, et al., *Nucl. Inst. Methods A* 355 (1995) 501–505.
- [6] T. Shintake, in: *Proc. of the 8th Symp. on Accel. Sci. and Technol., Ionics Pub., Tokyo, Japan, 1991*, pp. 290–292.
- [7] T. Shintake, et al., *Int. J. Mod. Phys. Proc. Suppl.* 2A (1993) 215–218.